THERMAL ENERGY STORAGE USING DESERT SAND: A NUMERICAL STUDY OF THE THERMOFLUIDIC PERFORMANCES

Mahfoudi N.*, Kheiri A., El Ganaoui M., Moummi A.
*Author for correspondence
Laboratoire de Génie Civil, Hydraulique, Développement Durable et Environnement, LAR-GHYDE, Université Mohamed Khider , BP 145 , RP , 07000 , Biskra , Algérie
Université de Lorraine, CNRS, LEMTA UMR 7536, 2 Rue Jean Lamour, Vandoeuvre-lès-Nancy, F-54500, France.
Université de Lorraine, Laboratoire d'Energétique de Longwy/LERMAB, IUT Henri Poincaré de Longwy, 186 rue de Lorraine 54400 Cosnes Et Romain
Laboratoire de Génie Civil, Hydraulique, Développement Durable et Environnement, LAR-GHYDE, Université Mohamed Khider , BP 145 , RP , 07000 , Biskra , Algérie

E-mail: nadjiba213@yahoo.fr

ABSTRACT

The Thermal Energy Storage (TES) enhances the availability of renewable energy plants. It reduces the mismatch between the production and the demand of the electric energy. However, the high cost of the TES leads to a high overall cost of the produced electric kWh. In the case of solar power plants built in Saharan regions, the use of sand as the storing medium in the TES is a priori a suitable technique that can solve this problem. In fact, the sand presents good physical and chemical properties and it is locally available with a very low cost. In this paper, a numerical study has been conducted to assess the thermal and fluidic performances of a fixed bed and of a fluidized bed by using sand as storing medium. The heat is transferred to, and from, the sand by air. 2D and 3D simulations are conducted. The temperature profiles of the bed are examined as well as the storing rates. Parametric studies with the air speed and the height of the bed were considered. The results gained in this paper indicate that it is very viable and promising to integrate sand as storing media in the solar thermal applications especially where this material is plentiful.

INTRODUCTION

Energy storage technologies are a necessary component for any efficient use of renewable energy sources. Among them, TES has attracted increasing interest for both thermal applications and power plants. Of the many materials available for sensible storing, the most commonly used are Water, Sand, Concrete and ground [1-4]. A promising sensible heat storing material must also be ecologic, inexpensive, and must have a good thermal diffusivity [5].

The advantages of TES systems using sand as a storage media, include very low cost of thermal energy storage media, high and timely stable heat transfer rates into (and out of) sand, easy handling operations. Recent studies in USA and Spain showed the interest of using sand as storing media [6,7]. S. Hassan et al. [8] shown that sand has suitable thermal properties and stands as a candidate for storing heat. El Sebaii et al. [9] investigated the effectiveness to use sand as a storage material in an active single basin solar still. They have found that the annual average of daily productivity with storage is 23.8% higher than that when is used without storage [9].

Thanks to its good thermal inertia, and its availability in a plentiful way in several regions of the world (North of Africa, Gulf states, America, Middle east…), it will be interesting to use sand as a storage medium [10-12].

Hence, in the present work, the thermal behavior and the storage performances of sensible TES using sand as the storing media is investigated using two technologies: fixed and fluidized bed.

NOMENCLATURE

C_d	[-]	Drag coefficient
C_p	[J/kg.K]	Specific heat
d	[m]	Diameter of solid phase
g	[m/s^2]	Acceleration due to gravity
h	[J/s.m.K]	Heat transfer coefficient between c and d phase
H	[kJ./kg]	Enthalpy
H_0	[m]	Initial height
k	[W/mK]	Thermal conductivity
L	[m]	Lenght of the fluidized bed
p	[Pa]	Pressure
t	[s]	Time
T	[K]	Temperature
u	[m/s]	Velocity
Q	[J]	Heat storage capacity
V	[m^3]	Sand Volume

Special characters

β	[-]	Inter-phase momentum exchange coefficient
μ	[Pa s]	Viscosity
ρ	[kg/m^3]	Density
Θ	[m^2/.s^2]	Granular temperature
Φ	[-]	Volume fraction
τ	[Pa]	Stress tensor

Subscripts

c	Continious (air)
ch	Charging
d	Dispersed (solid)
f	Fluid
ini	Initial
k	Phase k, continious or dispersed
s	Solid

THERMAL MODELING OF SENSIBLE HEAT STORAGE

Fixed bed

Figure 1 shows the physical model of the TES unit for numerical calculation. The storage unit is a regenerative type heat exchanger which absorbs/releases heat energy by passing the hot/cold Heat Transfer Fluid (HTF) respectively through the charging tubes. It consists of cubic bed with charging tubes embedded into it. The outer surface of the unit is well insulated to avoid heat losses to ambient environment.

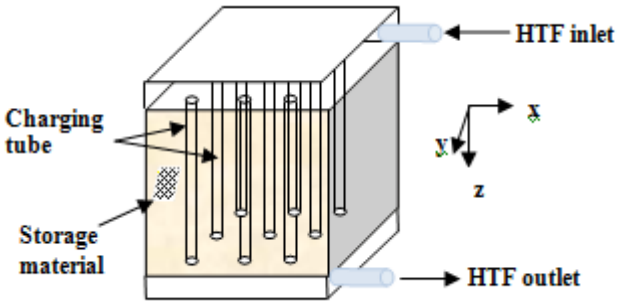

Figure 1. Physical model of sand heat storage fixed bed

While developing the thermal model for heat transfer the following assumptions were made:

- The HTF entering inside was laminar and fully developed.
- The sensible heat storage material is isotropic.
- The frictional pressure drop of HTF is neglected through the tubes.
- Laminar flow and adiabatic wall were assumed.
- Thermal proprieties, including density, of the fluid and of the sand were assumed constant
- Axial (z direction) conduction in HTF is neglected.

The HTF flow inside the charging tube is simulated by solving the continuity and the Navier-Stocks equation simultaneously.

$$\frac{\partial \rho_f}{\partial t} + \vec{\nabla}.(\rho_f \vec{v}) = 0 \qquad (1)$$

$$\rho_f \frac{D\rho_f}{Dt} = -\vec{\nabla}P + \mu\nabla^2\vec{u} \qquad (2)$$

The heat transfer from the HTF to the wall takes place by convection; the energy equation describing heat transfer process is given by (radiative transfer are neglected):

$$\rho_f C_{pf} \frac{DT_f}{Dt} = \lambda_f \nabla^2 T_f \qquad (3)$$

In the storing media, i.e. sand, the heat conduction equation to be solved stands as:

$$\rho_s C_{ps} \frac{\partial T_s}{\partial t} = K_S \nabla^2 T_s \qquad (4)$$

Furthermore, the tube thickness is neglected and as a boundary layer condition, the equality of the surface heat rates is considered between the HTF and the sand.

The heat storage capacity is calculated using:

$$Q = \rho_s V C_{ps} \Delta T_{ch} \qquad (5)$$

Where ΔT_{ch} is the sand temperature change since the storing starts. At the initial condition ($t = 0$), there is no flow of HTF through the charging tubes and all the domain is at uniform temperature T_{ini}. As illustrated in Figure 2, at the inlet of the tubes, there is a constant temperature T_{inlet} and a constant fluid velocity, at any time ($t > 0$). All the outer surfaces of the TES are well insulated.

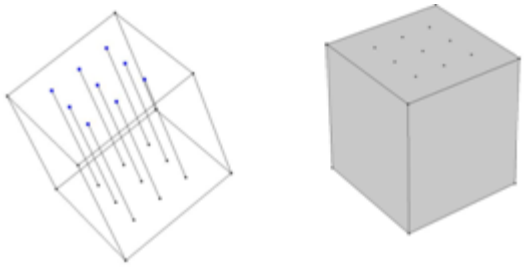

Inlet:

At (t = 0): $\vec{v} = 0$; $T = T_{ini}$

At (t > 0): $\vec{v} \neq 0$; $T = T_{inlet}$

Thermal insulation:

$n.(k \nabla T) = 0$;

n: is the normal vector.

Figure 2 Initial and boundary conditions of the model

Fluidized bed

The computational domain for simulation is shown in Figure 3. It is represented by a 2D planar with a width of L and a height of H. The initial height of packed bed of the dispersed phase (Sand) is H_0 when there is no fluid flow.

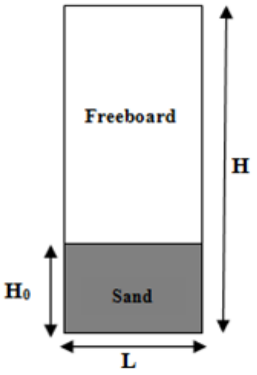

Figure 3 Study domain of sand fluidized bed

In the fluidized bed, the governing equations of the multiphase flow are:

Mass conservation for phase k (k = c for air and d for sand)

$$\frac{\partial}{\partial t}(\phi_k \rho_k) + \nabla.(\phi_k \rho_k u_k) = 0 \qquad (6)$$

with:

$$\sum_{k=1}^{n} \phi_k = 1 \qquad (7)$$

Where ϕ and ρ are respectively the volume fraction and the density of the phase k.
Momentum conservation for continuous phase:

$$\frac{\partial}{\partial t}(\phi_c \rho_c u_c) + \nabla.(\phi_c \rho_c u_c u_c) = -\phi_c \nabla p + \nabla.\bar{\bar{\tau}}_c + \phi_c \rho_c g - \beta_{cd}(u_c - u_d) \quad (8)$$

Momentum conservation for dispersed phase:

$$\frac{\partial}{\partial t}(\phi_d \rho_d u_d) + \nabla.(\phi_d \rho_d u_d u_d) = -\phi_d \nabla p - \nabla p_d + \nabla.\bar{\bar{\tau}}_d + \phi_d \rho_d g - \beta_{cd}(u_d - u_c) \quad (9)$$

Where u_k is the velocity of the phase k, P is the pressure, $\bar{\bar{\tau}}_k$ is the stress tensor of the phase k, and β_{cd} is the inter-phase momentum exchange coefficient.

Thermal energy conservation continuous phase:

$$\frac{\partial}{\partial t}(\emptyset_c \rho_c H_c) + \nabla.(\emptyset_c \rho_c u_c H_c) = -\nabla.\emptyset_c k_c \nabla T_d + h_{dc}(T_c - T_d) \quad (10)$$

Thermal energy conservation dispersed phase:

$$\frac{\partial}{\partial t}(\emptyset_d \rho_d H_d) + +\nabla.(\emptyset_d \rho_d u_d H_d) = -\nabla.\emptyset_d k_d \nabla T_d + h_{dc}(T_d - T_c) \quad (11)$$

Where H_k is the enthalpy of the phase k, k_k is the thermal conductivity of the phase k, h_{dc} is the heat transfer coefficient between c and d phases, and T_k is the temperature of the phase k.

The algebraic granular temperature was adopted [13]:

$$0 = (-p_d \bar{\bar{I}} + \bar{\bar{\tau}}_d) : \nabla u_d - \gamma_d - 3\beta_{cd}\theta_d \quad (12)$$

θ_d is the granular temperature.

Material property and simulation parameters used for the simulation are listed in Tables 1.

Table 1
Material properties of gas and solid phases and Simulation parameters

Flow type	Laminar
Gas-solid model	Euler-Euler, with kinetic theory
Time step used	*0.001 s*
Convergence criteria	*10-3*
Superficial gas velocity	*0.25 m/s*
Max. solid packing volume fraction	*0.60*
Initial air temperature	*473 K*
Initial sand temperature	*300 K*
Initial height of sand	*40 cm*
Sand heat capacity	*830 J.kg^{-1}.K^{-1}*
Sand density	*2650 kg.m^{-3}*
Sand particle diameter	*162 μm*

RESULTS AND DISCUSSION

The charging time for fixed bed is shown in Figure 4. It is seen that the sand bed takes about 10 days to be completely charged.
The variation of the thermal energy storage rate for the selected material is shown in Figure 5. The amount of the thermal energy stored at the charging time is calculated using Eq. 5. The energy stored in the sand fixed bed is 12.69 MJ. The energy storage rate of the bed is initially zero when there is no heat input and it rises with time till the storage bed is fully charged. Since the energy storage rate is function of volume average temperature of the storage bed, it has the same profile.

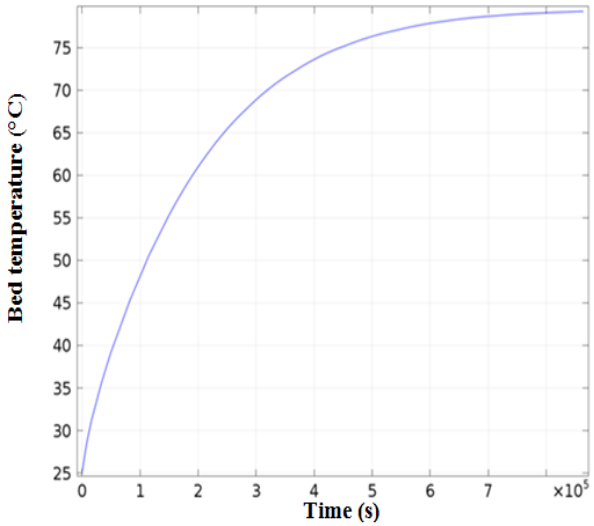

Figure 4 Charging time of sand fixed bed

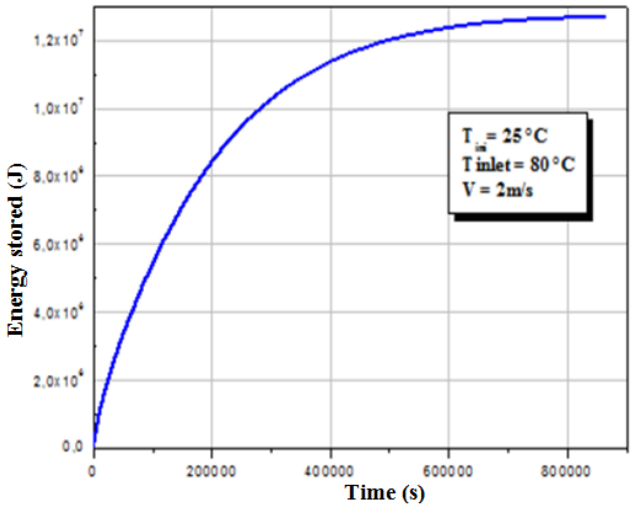

Figure 5 Rate of energy stored in sand fixed bed

In order to show the HTF temperature variation along the storage bed, HTF temperature is depicted along the central charging tube at a constant radial position at different intervals of charging time, 1 hour, 2 hours, 5 hours, and 24 hours (Figure 6). During the first hour of charging the temperature

drop of HTF is 12 °C. However, after 24 hours the temperature drop is about 0.1 °C.

Initially, the TES is at a temperature lower than T_{inlet} the storage is initiated by supplying HTF at temperature T_{inlet}. As a result, the HTF temperature drops along the charging tubes and exits at a lower temperature, T_{outlet}.

During the initial period of charging time, the temperature drop of HTF is dominant, after certain duration, its value is almost constant and no further drop in temperature is registered as storage temperature itself rises with time and the driving potential for conduction is reduced.

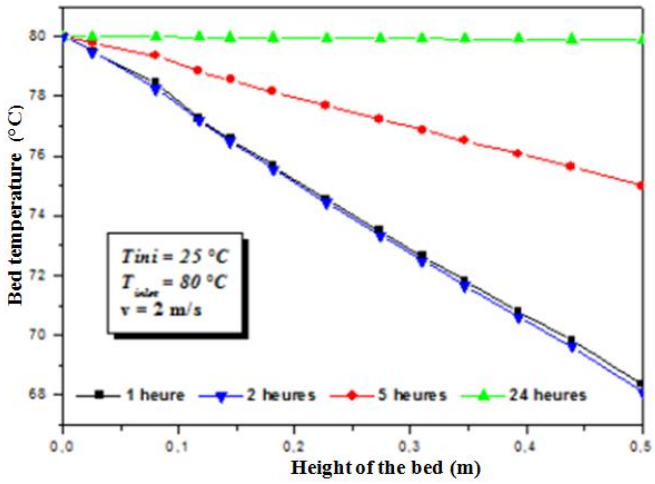

Figure 6 : Axial variation of HTF temperature in sand fixed bed

The effect of flow rate of HTF on charging time for sand is presented in Figure 7.

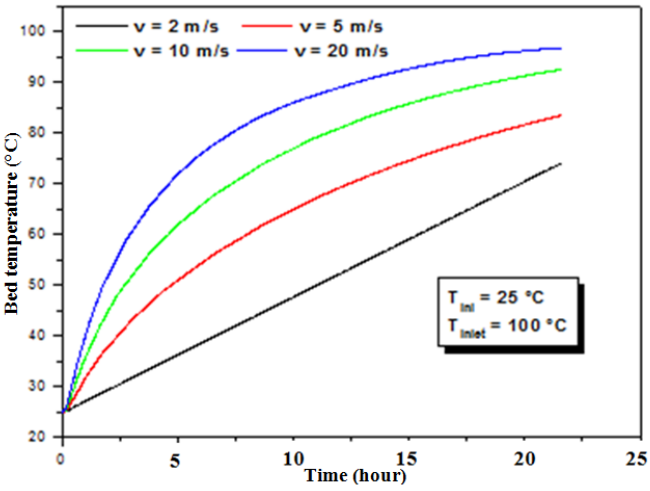

Figure 7 : Effect of HTF velocity on charging time of sand fixed bed

It is seen that the considerable reductions in charging times occur with increasing the mass flow rate of HTF (or velocity as cross section of tube is constant). Since, the increase in velocity of HTF leads to the improvement in convective heat transfer rate, the heat input to storage bed per unit time is higher so it takes less time to complete the charging cycle (ΔT_{ch}). The decrease in charging time of storage bed with HTF velocity of 2 m/s as compared to 10 m/s is higher than the decrease in charging time of storage bed with HTF velocity of 10 m/s as compared to 20 m/s. Hence, the increase in HTF velocity beyond 10 m/s will have less impact on the charging time of storage bed. Moreover increasing the HTF velocity causes more frictional pressure drop in the HTF and thus leads to more pumping power as the frictional pressure drop is proportional to the square of velocity of HTF fluid.

Concerning the thermal behaviour of the fluidized bed, Figure 8 shows the time variation of the mean dispersed phase temperature at eight of H = 15 cm in the sand fluidized bed. Note that, the average solid temperature shown is the mean of the particle temperature averaged across the section of the column at a given height. It is seen that for each time duration of about 1 minute, the sand temperature increases with gain of 6 °C. The fluctuations observed are due to the passage of the air bubbles through the bed allows both the cooling and the heating of the sand particle. It is shown that the hydrodynamic of the flow affects the thermal behaviour of the fluidized bed.

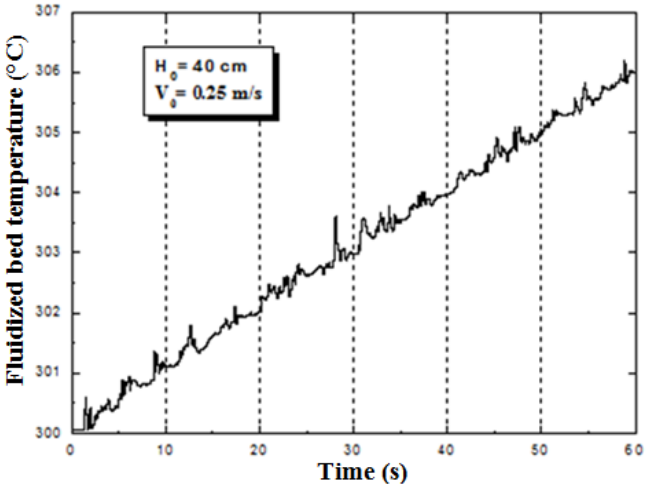

Figure 8 Variation of the temperature of the sand at height of H = 15 cm in the sand fluidized bed.

In order, to present the effect of the air velocity on the fluidized bed hydrodynamic, Figure 9 illustrates the expansion and the bubbles formation in the bed for different air velocities (0.25, 0.5 and 1 m/s). It has been seen that with the increase of the air superficial velocity, the bubbles sizes in the bed increase. At high velocities, a groups of a small bubbles are generated from the air distributor. Subsequently, the bubbles coalesce and produce then bigger structures as they move upwards and become stretched because of the interaction with other bubbles and because the bed wall effects.

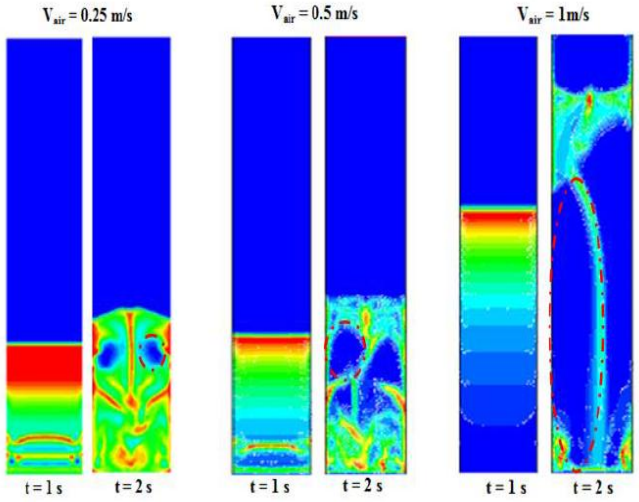

Figure 9 Effect of the air velocity on the hydrodynamic of the fluidized bed.

Figure 10 shows the variation of the solid phase temperature as function of the width of the fluidized bed at t = 45 s and for different height of the bed. It is seen that the temperature is uniform in all the bed. At this moment the chaotic regime is reached, promoting thus the heat exchanger in the fluidized bed.

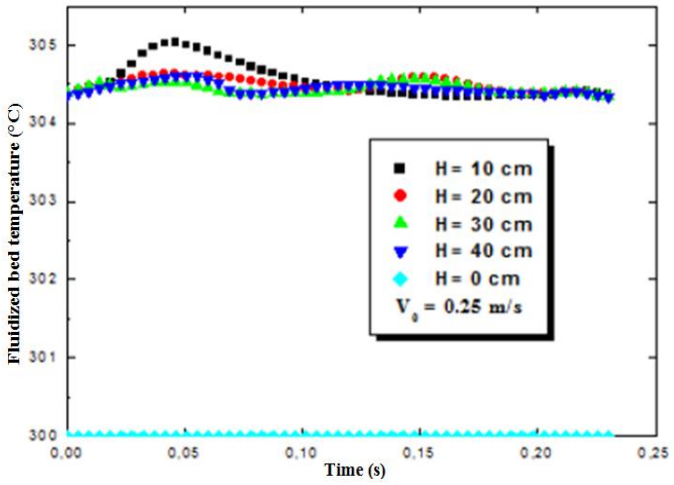

Figure 10 Variation of the temperature of the sand as function as the width of the fluidized bed.

CONCLUSION

In this paper, 2D and 3D simulation of sensible TES using desert sand, in fixed and fluidized bed were conducted to investigate its performances. For the fixed bed, a facility employing a configuration of nine charging tubes has been presented. It is found that the sand fixed bed takes about 10 days to be fully charged. In this case the capacity of storage is 12,96 MJ. The effect of HTF velocity on charging time of storage media has been analyzed.

For the fluidized bed, the results show that the hydrodynamic has an important effect on the thermal behaviour of the TES and thus on the storage capability. The chaotic formation of the bubbles allows a good heat transfer between the continuous phase (air) and dispersed phase (sand). This work is in progress to understand and compare the results with the first data obtained from an experimental TES with sand bed that is under construction in our laboratory.

REFERENCES

[1] A.I. Fernandez, M.Martınez , M.Segarra, I.Martorell, L.F.Cabeza, Selection of materials with potential in sensible thermal energy storage, *Solar Energy Materials & Solar Cells*, vol. 94, pp. 1723–1729, 2010.

[2] I. Dinçer, M. A. Rosen, Thermal Energy Storage Systems and Applications, 2nd ed., Willey, 2011, pp. 85–141.

[3] F. Bai, C. Xu, Performance analysis of a two-stage thermal energy storage system using concrete stream accumulator, *Applied Thermal Engineering*, vol. 31, pp. 2764-2771, 2011.

[4] M.E. Navarro, M.Martı´nez , A.Gil, A.I.Ferna´ndez , L.F.Cabeza, R.Olives, X.Py, Selection and characterization of recycled materials for sensible thermal energy storage, *Solar Energy Materials & Solar Cells*, vol. 107,pp. 131–135, 2012.

[5] M. Medrano, A. Gil, I. Martorell, X. Potau, L. Cabeza, State of the art on high-temperature thermal energy storage for power generation. Part 2—Case studies, *Renewable and Sustainable Energy Reviews*, vol. 14, pp. 56–72.2010.

[6] A. Gil , M. Medrano, I. Martorell, X. Potau, L. Cabeza, State of the art on high-temperature thermal energy storage for power generation. Part 1—Concepts, materials, and modelization, *Renewable and Sustainable Energy Reviews*, vol. 14, pp. 31–55, 2010.

[7] D. Fernandes, F. Pitié, G. Cáceres, J. Baeyens, Thermal energy storage: How previous findings determine current research priorities, *Energy*, vol. 39, 246-257, 2012.

[8] S. Hassan, R. S. Hernandez, K. Vonzabern, J. Pierce, K. Kantesaria, M. Rubin, Thermal Inertia of sand at different Levels of Water Saturation, *Proceedings of the 44th Lunar and Planetary science Conference*, Texas, 2013.

[9] A.A. El-Sebaii, S.J. Yaghmour, F.S. Al-Hazmi, Adel S. Faidah, F.M. Al-Marzouki, A.A. Al-Ghamdi, Active single basin solar still with a sensible storage medium, *Desalination*, vol. 249, pp. 699–706, 2009.

[10] N. Mahfoudi, A. Moummi, M. El. Ganaoui, Sand as a Heat Storage Media for a Solar Application: Simulation Results, *Applied Mechanics and Materials*, 621(214), 2014.

[11] N. Mahfoudi, A. Khachkouch, A Moummi B. Benhaoua, M. El Ganaoui, Design and characterization of a portable heat storage facility, *Mechanics & Industry*, 16 (4), pp 411-417, 2015.

[12] N. Mahfoudi, A. Moummi, M. El. Ganaoui, F. Mnasri, K. M. Aboudou, Simulation du comportement thermique d'un milieu poreux destinée au stockage sensible : Application à l'énergie solair, *Proceedings of the 3th* Colloque internationale Francophone d'énergétique et mécanique, Comores, PP. 91-99 5-7 Mai, 2014.

[13] M. Lungu, J. Wang, Y. Yang, Numerical simulation of flow structure and heat transfer in a central jet bubbling fluidized bed, *Powder technology*, PP. 139-152, 269 ,2015.